Astron. Astrophys. 356, 691–694 (2000)

ASTRONOMY AND ASTROPHYSICS

Research Note

Possible emission lines from the gaseous β Pictoris disk

A. Lecavelier des Etangs[1], L.M. Hobbs[2], A. Vidal-Madjar[1], H. Beust[3], P.D. Feldman[4], R. Ferlet[1], A.-M. Lagrange[3], W. Moos[4], and M. McGrath[5]

[1] Institut d'Astrophysique de Paris, CNRS, 98 bis Boulevard Arago, 75014 Paris, France
[2] University of Chicago, Yerkes Observatory, Williams Bay, WI 53191-0258, USA
[3] Université J. Fourier, Laboratoire d'Astrophysique, B.P. 53, 38041 Grenoble Cedex 9, France
[4] Johns Hopkins University, Department of Physics and Astronomy, Baltimore, MD 21218, USA
[5] Space Telescope Science Institute, 3700 San Martin Drive, Baltimore, MD 21218, USA

Received 23 March 1999 / Accepted 4 February 2000

Abstract. We present the results of exploratory HST observations to detect the emission lines of ions in the β Pictoris disk with the spectrograph slit placed off the star. Possible emission lines from Fe II have been detected at $\sim 10^{-14}$erg cm^{-2} s^{-1} at 0.5″ from β Pictoris, which would suggest a total Fe II density of $\gtrsim 2 \cdot 10^{-2}$cm^{-3} at 10 AU. This detection needs confirmation. If real, it requires a large production rate of gas and dust equivalent to the total disruption of ten bodies 30 kilometers in radius per year.

Key words: stars: individual: β Pic – stars: circumstellar matter – stars: planetary systems – methods: data analysis

1. Introduction

The β Pictoris disk is an evolved replenished circumstellar disk around a main sequence star, and appears to be a planetary (or cometary) disk (Vidal-Madjar et al. 1998). In addition to the dust disk, gas has been probed through absorption lines on the star line of sight (Lagrange et al. 1998). The observations of this gas component historically gave the most unexpected and important results with the detection of what appears to be the first extra-solar comets ever observed (Ferlet et al. 1987, Vidal-Madjar et al. 1998). However, non-radial motions are still unknown because observations are limited to the gaseous absorption lines on the star line of sight. Here we present the results of exploratory HST observations aimed to observe the emission lines of ions in the disk with the spectrograph slit off the star.

2. Observations and data analysis

2.1. Observations

The observations were made on February 9, 1996 with the HST/GHRS using the SSA slit (0.22″×0.22″) and echelle spectroscopy at an expected resolution of 80 000 to get the highest chance of detection of lines with *a priori* unknown width. After a peak-up on the star β Pictoris and the acquisition of reference spectra, the telescope was shifted to the south-west part of the β Pictoris disk at a position angle of 31.5 degrees to a distance of 0.5 and 1.5″ from the star. The log of the observations is summarized in Table 1. The candidate lines are those from ions for which strong absorptions have been seen in the stable component due to the gas disk and in the variable components due to the infalling comets. On this basis, we expected the strongest fluorescence.

Table 1. Log of the observations performed on Feb. 9$^{\rm th}$ 1996. r is the distance from β Pictoris

#	r	Wavelength (Å)	Lines	Time (UT)	T_{exp} (s)
1	0.0″	1803.1 - 1812.7	Ni II S I, Si II	08:39:03	230
2	0.0″	2373.0 - 2384.6	Fe II	08:46:42	173
3	0.5″	2373.0 - 2384.6	Fe II	08:55:45	2016
4	0.5″	1803.1 - 1812.7	Ni II S I, Si II	10:28:45	2073
5	1.5″	1803.1 - 1812.7	Ni II S I, Si II	11:58:39	3571
6	0.5″	1652.7 - 1661.2	C I C I*, C I**	14:46:39	2534

2.2. The method

The spectra observed on the disk present the same general shape as the spectra on the star but with a lower intensity level. Indeed, any spectrum of the disk obtained off the star ($F_{obs}(\lambda)$) is an addition of a "noise" component and a spectrum carrying information from the disk at the pointed position. The "noise" is the spectrum of the starlight scattered by the telescope ($aF_*(\lambda)$, where $F_*(\lambda)$ is the star spectrum) plus a background level (b) due to the fact that the background determined by the HST

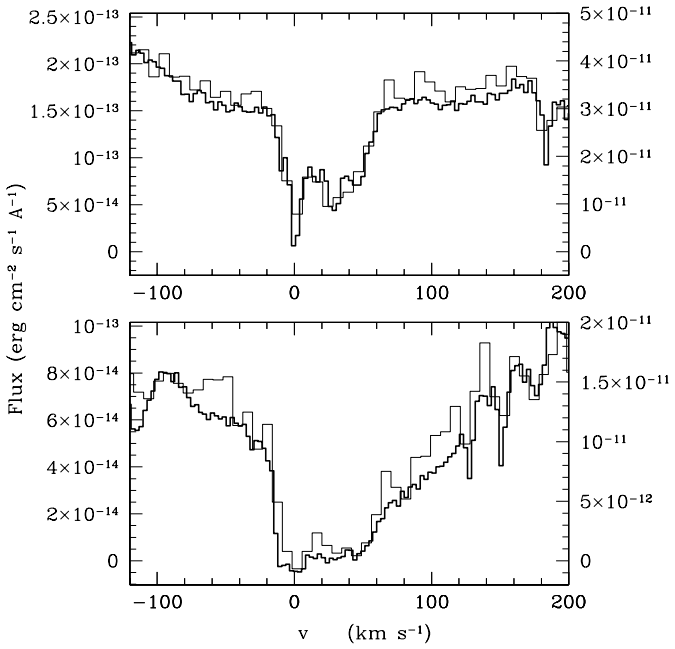

Fig. 1. Plot of the disk spectrum (thin line, left axis) and the star spectrum (thick line, right axis) in the region of the Fe II lines at 2374.461 Å (top panel) and 2382.765 Å (bottom panel). The velocities are relative to β Pictoris (21 km s^{-1} heliocentric). The data on the disk have been rebinned by 5 pixels, the data on the star by 2 pixels. The ratio of the right axis to the left axis is 197.

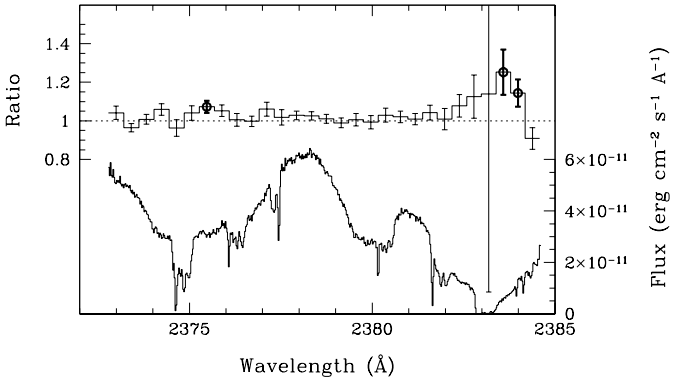

Fig. 2. Ratio of the disk spectrum to the star spectrum (top histogram, left axis) and plot of the star spectrum #2 (bottom spectrum, right axis). The pixels have been rebinned in boxes of 50 km s^{-1}width. To evaluate the ratio, the disk spectrum has been rescaled with $a^{-1} = 197$ and $b = 3 \cdot 10^{-15}$ erg cm^{-2} s^{-1} Å^{-1}. The errorbars are at 1σ level. The points from which a signal is detected at 2σ are plotted in bold. The dip in the spectrum between 2377 Å and 2378 Å is due to hot diodes. An excess emission is detected in the red part of the two strongest Fe II lines.

pipeline can be slightly miscalculated. The part of the spectrum due to the disk (F_{disk}) is the starlight scattered by the dust and the possible emission lines due to gaseous fluorescence. We thus consider that the additional noisy component (F_{noise}) is a linear combination of the stellar spectra ($F_*(\lambda)$) obtained at the same wavelength a few orbits before:

$$\begin{aligned} F_{obs}(\lambda) &= F_{noise}(\lambda) + F_{disk}(\lambda) \\ &\approx aF_*(\lambda) + b + F_{disk}(\lambda). \end{aligned} \quad (1)$$

To put forward the potential presence of a component different from the dominant starlight scattered by the telescope, we divide the observed spectra by the stellar spectra. The presence of a disk contribution at a wavelength λ will be detected if the ratio $F_{obs}(\lambda)/(aF_*(\lambda) + b)$ is significantly different from 1.

The main problem is thus the determination of a and b, and their errorbars within a confidence level. Assuming that the disk spectra (dust scattered light plus gas emission lines) have a negligible contribution to the observed spectra ($F_{noise}(\lambda) \gg F_{disk}(\lambda)$), we can determine a and b by a χ^2 minimization of

$$\chi^2 = \sum_{\lambda_i} w_{\lambda_i}(aF_*(\lambda_i) + b - F_{obs}(\lambda_i))^2, \quad (2)$$

where $w_{\lambda_i} = 1/\sigma^2_{\lambda_i}$ is the weight of each measurement at λ_i. This procedure gives not only the best determination of a and b but also intervals of confidence for these constants.

2.3. Results in the Fe II lines

Spectra in the Fe II wavelength range were obtained less than 10 minutes apart with the same instrument setting. The star and the disk spectra can be easily superimposed as shown in Fig. 1. An excess of flux clearly appears in the blue *and* the red part of the two strongest Fe II lines at rest wavelength 2374.461 Å and 2382.765 Å. If a and b are determined as described in Sect 2.2, we get $a^{-1} = 197 \pm 3$ and $b = (3 \pm 2) \cdot 10^{-15}$ erg cm^{-2} s^{-1} Å^{-1}. With these parameters, a plot of the ratio of the disk to the star spectra reveals an excess emission at 2σ level (Fig. 2). The flux from the disk can be evaluated by the difference between the two spectra ($F_{obs}(\lambda) - (aF_*(\lambda) + b)$), and is $F_{disk} \sim 10^{-14}$ erg cm^{-2} s^{-1} Å^{-1} between 50 and 150 km s^{-1} in the red part of the lines and around -50 km s^{-1} in the blue part (Fig. 3). This emission is about 1 Å wide and stronger in the red part of the lines.

2.4. Discussion

The detection of apparent excess emission in the two Fe II lines can be explained in different ways. We propose that this can be a real detection of the emission through the scattering of the starlight by the Fe II ions in very high velocity motions. This will be discussed in detail in the next section. However other possibilities must be evaluated.

First, this feature obviously cannot be simply due to a possible miscalculation (underestimate) of b, the background correction. Indeed, by underestimating b, we could find false emission-like features at wavelength where the flux is low. But, one should increase the estimate of b above its 4σ upper limit ($8 \cdot 10^{-15}$ erg cm^{-2} s^{-1} Å^{-1}) to explain the detected emission feature only by this effect. In addition, the emission is detected in both Fe II lines, in particular in the Fe II line at 2374.461 Å

where the level is far above the zero level, and for which an error on the estimate of b has almost no effect on the result. In fact, b is well-determined by the very bottom of the strongest Fe II lines where the level is clearly less than $1 \cdot 10^{-14}$ erg cm^{-2} s^{-1} Å^{-1} (Fig. 1).

However, apparent emissions due to the addition of the statistical noise and a bad estimate of the background level might be possible. But, although not excluded, it is very unlikely that this coincidence can contribute to give apparent emissions in the two sides of the two strongest Fe II lines.

The most important alternative to emission by Fe II is a time variation of the β Pictoris spectrum between the observations of the template (the star) and the disk spectra. If the absorption component in the Fe II lines had significantly decreased during the acquisition of the data, then the result is an apparent excess of emission in the second spectrum obtained with the slit off the star. Although the time between both spectra has been minimized, this possibility cannot be excluded without new observations, for example on the other side of the disk where the emission should be stronger in the blue.

3. The Fe II emission lines

3.1. The dynamics of the Fe II ions

If this detection is really due to emission by Fe II ions, the lines width must be explained through the dynamics of these Fe II ions in the disk. The Fe II ions must be ejected from the β Pictoris system by the radiation pressure which is stronger than the gravitation by a factor $\beta_{FeII} \approx 5$ (Lagrange et al., 1998). After ejection, they rapidly reach a constant asymptotic velocity v_∞. If they are ejected from a body on a circular orbit, $v_\infty \sim \sqrt{(2\beta - 1)(GM/a_0)}$, where a_0 is the radius of the orbit of the parent body. If they are ejected from a comet on a parabolic orbit, the final velocity is $v_\infty \sim \sqrt{(2\beta GM/a_0)}$. In this simple scheme, the observed final velocity of about 100 km s^{-1} (Fig. 3) corresponds to a production at about 1.5 AU from the star, or similarly to the absence of gas drag beyond that distance.

The emission lines are stronger in the red than in the blue. This is similar to the asymmetry already observed in the cometary absorption lines which are mainly redshifted (Beust et al. 1996), and well-explained by the evaporation of comets with a small range of longitude of periastron (Beust et al. 1998). But the "stable component" of the gas disk observed for example in Ca II and Fe II ions is found at zero radial velocity; a dragging torus of gas is needed to support the radiation pressure on these ions (Lagrange et al. 1998, Beust et al. 1998).. Even if the production of Fe II is not axisymmetric, these ions could be redistributed within this torus. Thus, an alternative explanation for the observed asymmetry in the emission lines could be an extended shape for this torus. The Fe II ions should be trapped in this torus and then progressively released on hyperbolic orbits when radiation pressure starts to dominate the gas drag. If this torus extends to several (~ 5) AU, and if the disk is observed in the "red side", the observed ions are still partly sensitive to the torus rotation and the amount of emission by redshifted ions must be larger than by the blueshifted ions (Fig. 4). Anyway, it is clear that the observed south-west branch of the disk must be the "red side" of the disk (Fig. 4). This provides an observational test: the north-east branch must present a larger emission in the blue lines.

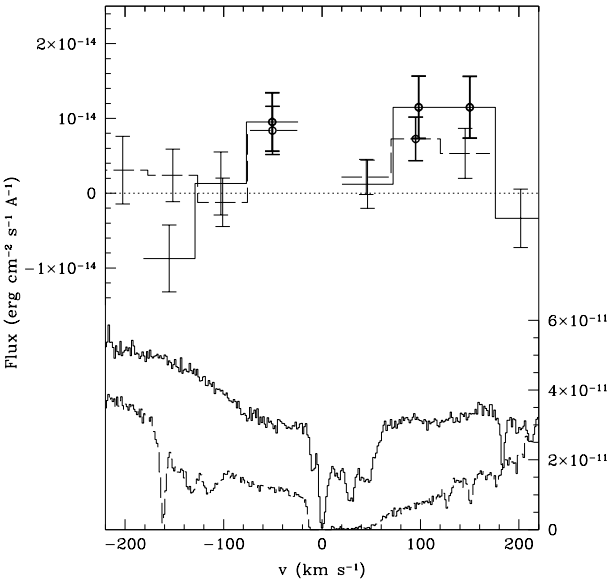

Fig. 3. Plot of the Fe II emission in the disk spectrum at 0.5″ obtained by the subtraction of the star scattered light (top histogram, solid line for the 2374.461 Å Fe II line and dashed line for the 2382.765 Å Fe II line, left axis). The data have been rebinned in boxes of 50 km s^{-1} wide. Abscissa are radial velocities relative to the radial velocity of the star, i.e. heliocentric minus 21 km s^{-1}. The errorbars are at 1σ level. The points for which a signal is detected at 2σ are plotted in bold. The two bottom spectra are β Pictoris spectra (right axis). Because of the strong Fe II absorption lines of the stable disk (at 0 km s^{-1} relative to β Pictoris, 21 km s^{-1} heliocentric), pixels with a velocity between -25 km s^{-1} and $+20$ km s^{-1} relative to β Pictoris are very noisy and are not taken into account. The two Fe II lines give about the same emission although their shapes and their levels are very different.

3.2. The Fe II density

The total brightness of Fe II emission lines can be evaluated to be:

$$F_{emission} = \frac{\Omega d^2 s F_\nu^{\beta\mathrm{Pic}}}{4\pi} \int n(r)/r^2 dx \qquad (3)$$

in erg cm^{-2} s^{-1}, where Ω is the solid angle covered by the spectrograph slit. The SSA slit (0.22″x0.22″) gives $\Omega = 10^{-12}$. d is the distance to β Pictoris ($d = 19.3$ pc$\approx 6 \cdot 10^{19}$cm). s is the frequency integral of the cross section. $F_\nu^{\beta\mathrm{Pic}}$ is the brightness per unit of frequency of β Pictoris seen from the Earth at the relevant wavelength. $n(r)$ is the density of the observed ion at a distance r from the central star. dx is the differential length along the line of sight. We can define a weighted integral equivalent to the column density by

$$\tilde{N}_{r_0} \equiv \int \frac{n(r)}{r^2} r_0^2 dx = \frac{4\pi r_0^2 F_{emission}}{\Omega d^2 s F_\nu^{\beta\mathrm{Pic}}}, \qquad (4)$$

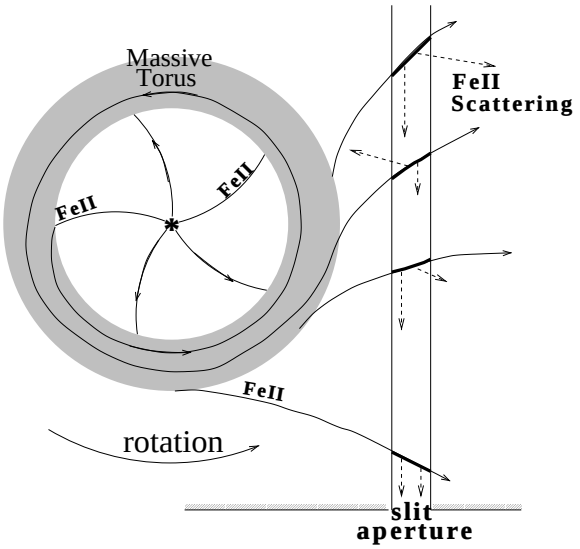

Fig. 4. Sketch of the possible dynamics of the β Pictoris disk. FeII ions are produced close to the star, spiral into a massive torus and then cross the line of sight defined by the slit. We see the resonant scattering through emission lines blueshifted and redshifted by the radiation pressure. The observed larger amount of redshifted Fe II is due either to the rotation of the massive torus which drags these Fe II ions, or to an asymmetrical production of ions as inferred from the falling comets scenario. In summary, the large velocities are due to the radiation pressure, and the asymmetry between the red and the blue is due to the rotation of the system.

where r_0 is the impact parameter of the line of sight ($r_0(0.5'') = 10$ AU). For the Fe II 2382 Å line, $s = 8 \cdot 10^{-3}$ cm^2 s^{-1} and the observed emission is $F_{emission} = F_\lambda^{disk} \Delta\lambda \sim 10^{-14}$erg cm^{-2} s^{-1}. Finally, we have

$$\tilde{N}_{10\mathrm{AU}} \cong 5.2 \cdot 10^{26} \left(\frac{F_{emission}}{\mathrm{erg\ cm^{-2}\ s^{-1}}} \right) \mathrm{cm}^{-2} \quad (5)$$

$$\tilde{N}_{10\mathrm{AU}} \sim 5 \cdot 10^{12} \mathrm{cm}^{-2} \quad (6)$$

This value is consistent with the Fe II column density ($N_{\mathrm{Fe\ II}} = \int n(r)dr = 3 \cdot 10^{14}$ cm^{-2}) and the hypothesis that Fe II should be gathered in the dragging torus around 1 AU and that they have an r^{-2} distribution beyond this torus (Lagrange et al. 1998). To evaluate the Fe II volume density, n_0, at r_0, we can define the dimensionless quantity K by $K \equiv \int n(r) r_0/(n_0 r^2) dx$. Then,

$$n_0 = \frac{4\pi r_0 F_{emission}}{\Omega d^2 s F_\nu^{\beta\mathrm{Pic}} K} = \frac{\tilde{N}}{r_0 K}. \quad (7)$$

If we make the assumption that $n(r) = n_0 (r_0/r)^\alpha$, we have $K_{\alpha=0} = \pi$, $K_{\alpha=1} = 2$, $K_{\alpha=2} = \pi/2$,..., $K_{\alpha=8} = 35\pi/128$, *et cetera*. $\alpha = 2$ would correspond to gas expelled by radiation pressure. For reasonable value of α, within a factor of 2, $K \sim 2$. As a final result, we get

$$n_0 \sim 2 \cdot 10^{-2} \mathrm{cm}^{-3}, \quad \mathrm{at}\ \sim 10\ \mathrm{AU}. \quad (8)$$

The calculation has been done with the hypothesis of an optically thin line. We also assume that the filling factor in the vertical direction is 1, thus the obtained density n_0 is in fact a lower limit. The other Fe II line at 2374 Å has an oscillator strength 10 times smaller but the stellar flux is larger at this wavelength ($\sim 4 \cdot 10^{-11}$ erg cm^{-2} s^{-1} Å^{-1}). It gives about the same value of density within a factor of 2.

The corresponding Fe II production rate can be roughly estimated by the flux of material ($v = 100$ km s^{-1}) through the area observed at 10 AU with high $H(0.22'') = 4.4$ AU: $Q(\mathrm{Fe\ II}) = 2\pi r_0 H v n_0 \approx 10^9$ kg s^{-1}. With solar abundances, this corresponds to the total disruption of about 10 planetesimals per year with a radius of 30 km. Here must be mentioned that cold CO has been detected in the β Pictoris disk and the inferred CO production rate is about 10^{11} kg s^{-1} (Vidal-Madjar et al. 1994, Lecavelier des Etangs 1998).

4. Need for confirmation

To confirm the tentative detection presented in this paper, new observations are really needed. The first obvious method will be to observe the other (north-east) side of the disk which should present the same feature except blueshifted instead of redshifted. We can also observe other lines which should present the same characteristics. The Fe II lines at 2600 Å and Mg II lines at 2800 Å are well-suited candidates. The Cr II line at 2050 Å with an intermediate $\beta_{\mathrm{Cr\ II}} \approx 3$ is also an interesting target (Lagrange et al. 1998). STIS, with long-slit capability is technically better suited to this observation.

5. Conclusion

HST observations planned to detect the emission lines of ions in the β Pictoris disk with the spectrograph slit placed off the star gave a marginal detection of possible emission lines from Fe II ions at 0.5″ from β Pictoris. This would suggest an Fe II density of $\sim 2 \cdot 10^{-2}$cm^{-3} at 10 AU.

If real, this indicates a large production rate of gas and dust equivalent to the total disruption of 10 bodies of 30 kilometers in radius per year. This corresponds to a production rate of about $2 \cdot 10^{-7} \mathrm{M}_{\mathrm{Earth}}$ per year. New observations are obviously needed to confirm this detection.

Acknowledgements. We thank M. Deleuil, C Gry and J.J. Lissauer for their help in this work. We would like to express our gratitude to Ramana Athreya for his help with the figures. This work was financially supported in part by grant GO-05881.01-94A from the Space Telescope Science Institute to the University of Chicago.

References

Beust H., Lagrange-Henri A.M., Plazy F., Mouillet D., 1996, A&A 310, 181
Beust H., Lagrange A.-M., Crawford I.A., et al., 1998, A&A 338, 1015
Ferlet R., Hobbs L.M., Vidal-Madjar A., 1987, A&A 185, 267
Lagrange A.-M., Beust H., Mouillet D., et al., 1998, A&A 330, 1091
Lecavelier des Etangs A., 1998, A&A 337, 501
Vidal-Madjar A., Lagrange-Henri A.-M., Feldman P.D., et al., 1994, A&A 290, 245
Vidal-Madjar A., Lecavelier des Etangs A., Ferlet R., 1998, Planet. Space Sci. 46, 629